DOI: 10.24874/ti.2070.11.25.03

Tribology in Industry

www.tribology.rs

RESEARCH

Semi-Empirical Modeling of Surface Roughness in Turning

Miroslav Radovanović[a,*]

[a]University of Niš, Faculty of Mechanical Engineering, Beogradska 14, 18000 Niš, Serbia.

Keywords:

Turning
Surface roughness
Semi-empirical model
Dimensional analysis
Buckingham's π theorem
Design of experiments

* Corresponding author:

Miroslav Radovanović
E-mail:
miroslav.radovanovic@masfak.ni.ac.rs

Received: 17 November 2025
Revised: 23 December 2025
Accepted: 23 March2026

A B S T R A C T

The study presents a novel semi-empirical dimensionless mathematical model for predicting surface roughness (Ra) in the finish turning of AISI 316LVM stainless steel. The proposed model integrates dimensional analysis (DA), design of experiments (DoE), and regression analysis (RA) to obtain a realistic and industrially applicable model. Dimensional analysis was applied to derive a dimensionally homogeneous mathematical model. Buckingham's π theorem was used to express the relationship between surface roughness and the influencing factors in dimensionless form. As a result, the normalized surface roughness $Ra/(f^2/r_\varepsilon)$ is expressed as a function of the normalized cutting parameters: $a_p/a_{p,rec}$, f/f_{rec}, and $v_c/v_{c,rec}$, which are normalized with respect to the tool manufacturer's recommendations. Taguchi's design of experiments and analysis of variance (ANOVA) were used to investigate the effects of four process factors (corner radius, depth of cut, feed, and cutting speed) on surface roughness. Regression analysis was then used to determine the unknown coefficient and exponents in the mathematical model. The proposed approach is physically consistent and industrially relevant, providing a practical framework for developing predictive surface roughness models in turning operations.

1. INTRODUCTION

Machining is a fundamental manufacturing process used to produce parts by removing material from a workpiece in order to achieve the desired shape, dimensional accuracy, and surface quality. Among various machining processes, turning is the most widely employed, particularly for the production of rotationally symmetric parts. In turning operations, a single-point cutting tool removes material from a rotating workpiece, generating cylindrical, conical, and contoured surfaces, as well as threads and end faces. The primary motion is the rotation of the workpiece, while the secondary motion is the linear feed of the cutting tool. The process is carried out on a lathe and requires a cutting tool, workpiece, and appropriate clamping systems to secure both the tool and the workpiece. Turning performance is usually determined by multiple interrelated process factors, such as depth of cut, feed, and cutting speed. Engineers are constantly

trying to optimize these factors to increase productivity, reduce costs, and improve surface quality. Among these objectives, surface quality is a critical characteristic, as it influences on functional performance of the part. Therefore, the prediction of surface quality is essential for process optimization. Surface quality, refers to the geometric and microstructural characteristics of machined surface. It comprises four primary components: roughness, waviness, lay, and flows. Among these, surface roughness is the most commonly measured and controlled characteristic. Surface roughness refers to the fine, short-wavelength irregularities on a machined surface. It is typically quantified using parameters such as the roughness parameters *Ra* and *Rz*, as defined by international standards [1]. In turning, surface roughness is influenced by a complex interaction of numerous factors. These factors can be systematically categorized as: tool-related factors (corner radius, cutting edge geometry, tool material and coating), workpiece-related factors (material type, hardness, microstructure), cutting parameters (depth of cut, feed, cutting speed), process factors (tool wear, vibration, temperature), machine tool characteristics (rigidity, dynamic stability), and environmental conditions (use of coolant, chip evacuation). Extensive research has been devoted to modeling surface roughness in machining. Numerous modeling approaches have been proposed, ranging from theoretical to empirical models. Theoretical models, such as the classical circle model for rounded-tip tools, provide fundamental relationships, but neglect effects such as tool wear and vibration. Empirical models, based on Response Surface Methodology (RSM), Artificial Neural Networks (ANN), and Regression Analysis (RA), are derived from experimental data and can achieve high accuracy within specific testing ranges; however, they often lack dimensional consistency. To address the limitations of both approaches, hybrid models have been developed, combining theoretical knowledge with empirical data to enhance prediction accuracy and robustness. For instance, a hybrid model may combine a theoretical base structure with an empirical or AI-based component, such as an artificial neural network (ANN), to capture the complex residuals arising from factors like vibration and tool wear. However, these hybrid models rarely incorporate dimensional analysis, which is essential for developing dimensionally consistent models.

The application of dimensional analysis to modeling machining processes is rarely reported in the literature. Several studies have applied dimensional analysis (DA) to develop mathematical models for turning processes, including surface roughness [2], cutting force [3] tool life [4], and material removal rate [5]. A review of the literature shows that existing dimensionless models in turning do not include cutting parameters normalized with respect to tool manufacturer's recommendations. In industrial machining practice, however, tooling catalogs commonly provide recommended values for depth of cut ($a_{p,rec}$), feed (f_{rec}), and cutting speed ($v_{c,rec}$), which are established based on extensive experimental investigations.

This study presents a novel semi-empirical dimensionless model for predicting surface roughness in the finish turning of AISI 316LVM stainless steel, which uses the tool manufacturer's recommended values as reference levels. The model integrates dimensional analysis (DA) via Buckingham's π theorem to derive a dimensionally homogeneous model form, design of experiments (DoE) using the Taguchi method to investigate the effects of factors, and regression analysis (RA) to determine empirical constants and coefficients. The proposed semi-empirical model expresses the normalized surface roughness $Ra/(f^2/r_\varepsilon)$ as a function of the normalized cutting parameters: $a_p/a_{p,rec}$, f/f_{rec}, and $v_c/v_{c,rec}$, which are normalized with respect to the tool manufacturer's recommendations. This methodology ensures dimensional consistency, and enables practical industrial use.

2. LITERATURE REVIEW

Despite the advantages of hybrid approaches, the literature is still dominated by purely empirical work. Many studies have traditionally examined surface roughness in turning and proposed mathematical models. These studies analyze the influence of various factors such as workpiece material, tool material, and cutting parameters (e.g., depth of cut, feed, and cutting speed) on surface roughness. As a result, they usually present empirical models for surface roughness prediction, which are derived from and

applicable to the specific conditions tested. This review considers only those studies that include, among other factors, corner radius and feed as control factors, with the aim of identifying both the selected factors and the forms of the proposed models. Models based on artificial neural networks (ANNs) or hybrid models were not considered.

Table 1. Overview of literature on surface roughness in turning.

Year	Authors	Workpiece Material	Tool Material	Control Factors	Experim. Design	Significant Factors	Empirical Model
2007	Singh, D., & Rao, P.V. [6]	Steel AISI 52100	Mixed ceramic	r_ε (0.4, 0.8, 1.2 mm) f (0.1, 0.2, 0.32 mm/rev) v_c (100, 150, 200 m/min) γ (6, 16, 26°)	Full factorial design	r_ε, f, v_c	Power
2015	Qehaja, N.; et al. [7]	Steel C62D	Coated carbide	r_ε (0.4, 0.8, 1.2 mm) f (0.178, 0.214, 0.285) mm/rev t_c (1700, 2590, 3950 s)	Full factorial design	r_ε, f, t_c	Power
2016	Dinesh, S.; et al. [8]	Steel EN 24	Coated carbide	r_ε (0.8, 2.2 mm) a_p (0.4, 0.8, 1.2, 1,6 mm) f (0.1, 0.15, 0.2, 0.25 mm/rev) v_c (110, 165, 210, 275 m/min)	Taguchi design L16	$r_\varepsilon, a_p, f, v_c$	Linear with interactions
2016	Izelu, C.O., & Eze, S.C. [9]	41Cr4	Carbide	r_ε (0, 1, 2 mm) a_p (1, 2, 3 mm) f (0.15, 0.20, 0.30 mm/rev)	Central composite design (CCD)	r_ε, a_p, f	Quadratic
2018	Medour, I.; et al. [10]	Steel AISI 4140, 60 HRC	Mixed ceramic	r_ε (0.8, 1.2, 1.6 mm) a_p (0.1, 0.2, 0.3 mm) f (0.08, 0.11, 0.14 mm/rev) v_c (120, 182, 244 m/min)	Box-Behnken design (BBD)	r_ε, f	Quadratic
2018	Patole, P., & Kulkarni, V. [11]	Steel AISI 4340, BHN 217	Coated carbide	r_ε (0.4, 0.8 mm) a_p (0.5, 1, 1.5 mm) f (0.04, 0.06, 0.08, 0.1, 0.12 mm/rev) v_c (75, 90 m/min)	Full factorial design	r_ε, f, v_c	Quadratic
2018	Zerti, O.; et. al. [12]	Steel AISI D3	Mixed ceramic	r_ε (0.8, 1.2, 1.6 mm) a_p (0.15, 0.3, 0.45 mm) f (0.08, 0.12, 0.16 mm/rev) v_c (220, 307, 440 m/min) κ (45, 75°)	Taguchi design L18	$r_\varepsilon, a_p, f, \kappa$	Linear with interactions
2019	Patel, V.D. & Gandhi, A. H. [13]	Hardened steel AISI D2	Cubic boron nitride (CBN)	r_ε (0.4, 0.8, 1.2 mm) f (0.04, 0.12, 0.2 mm/rev) v_c (80, 116, 152 m/min)	Full factorial design	r_ε, f, v_c	Power
2019	Saidi, R.; et al. [14]	Stellite 6	Coated carbide	r_ε (0.2, 0.4, 0.8 mm) a_p (0.15, 0.30, 0.45 mm) f (0.08, 0.12, 0.16 mm/rev) v_c (30, 55, 80 m/min)	Taguchi design L27	r_ε, a_p, f	Quadratic
2020	Ozdemir, M.; [15]	Steel St 37	Coated carbide	r_ε (0.4, 0.8, 1.2 mm) a_p (0.5, 1, 1.5 mm) f (0.1, 0.2, 0.3 mm/rev) v_c (150, 200, 250 m/min)	Taguchi design L27	r_ε, a_p, f	Quadratic
2020	Frifita, W.; et al. [16]	Inconel 718	Coated carbide	r_ε (0.4, 0.8 mm) f (0.08, 0.11, 0.14 mm/rev) v_c (34, 47, 70 m/min)	Taguchi design L18	r_ε, f, v_c	Linear with interactions
2020	Ky, L.H. [17]	Steel SAE 420	Coated cubic boron nitride (CBN)	r_ε (0.1, 0.2, 0.3, 0.4, 0.5 mm) a_p (0.05, 0.1, 0.15, 0.2, 0.25 mm) f (0.02, 0.04, 0.06, 0.08, 0.1 mm/rev) v_c (100, 140, 180, 220, 260 m/min)	Central composite design CCD	r_ε, f, v_c	Quadratic
2022	Tomov, M.; et al. [18]	Steel EN C55 (AISI 1055), 53 HRC	Cubic boron nitride (CBN)	r_ε (0.4, 0.8, 1.2 mm) a_p (0.2, 0.283, 0.4 mm) f (0.09, 0.134, 0.2 mm/rev) v_c (100, 141.4, 200 m/min)	Full factorial design	r_ε, f	Power
2023	Lu, J.; et al. [19]	Steel AISI 1045	Coated carbide	r_ε (0.4, 0.8, 1.2 mm) a_p (0.5, 1, 1.5 mm) f (0.15, 0.2, 0.25 mm/rev) v_c (120, 150, 180 m/min)	Box-Behnken design (BBD)	r_ε, f	Linear

Table 1 summarizes research on surface roughness in turning, including workpiece and tool materials, control factors, experimental design, significant factors, and empirical models.

Singh and Rao [6] investigated surface roughness in the hard turning of AISI 52100 steel with mixed ceramic cutting tools. A full factorial experimental design was implemented, incorporating four control factors: cutting speed, feed, effective rake angle, and corner radius. Analysis of variance (ANOVA) revealed feed as the most significant factor, followed by corner radius and cutting speed. A predictive model was developed using response surface methodology (RSM). The resulting non-linear regression model, formulated as a power-law equation, lacks dimensional consistency. Qehaja et al. [7] investigated surface roughness in the dry turning of cold-rolled C62D steel with coated carbide cutting tools, employing a three-level full factorial experimental design. Analysis of variance (ANOVA) indicated that feed, corner radius, and machining time were statistically significant. A predictive surface roughness model was developed using multiple regression analysis (RA) combined with response surface methodology (RSM) and was formulated as a power-law equation. However, the model lacks dimensional consistency. Dinesh et al. [8] investigated the optimization of surface roughness in the CNC turning of EN24 alloy steel with coated carbide cutting tools. The experiments were designed using a Taguchi L16 orthogonal array to examine the selected control factors: corner radius, depth of cut, feed, and cutting speed. Analysis of variance (ANOVA) revealed that feed is the most dominant factor influencing surface roughness. Using response surface methodology (RSM), a predictive model was developed in the form of a linear regression equation with interactions. While the resulting model was statistically adequate, it lacks dimensional consistency. Izelu and Eze [9] investigated surface roughness in the hard turning of 41Cr4 alloy steel with carbide cutting tools. The influence of depth of cut, feed, and corner radius was evaluated using a central composite design (CCD) within the framework of response surface methodology (RSM). Analysis of variance (ANOVA) revealed that feed and corner radius had the most significant influence on surface roughness. A quadratic regression model was developed, demonstrating high predictive accuracy within the experimental domain. However, as is typical of empirical RSM-based models, the resulting equation lacks dimensional consistency. Meddour et al. [10] investigated surface roughness in the hard turning of AISI 4140 steel (60 HRC) with mixed ceramic cutting tools using a Box–Behnken design. Cutting speed, feed, depth of cut, and corner radius were selected as control factors. Analysis of variance (ANOVA) revealed feed and corner radius as the significant factors, whereas cutting speed had a limited influence on surface roughness. A purely statistical quadratic model was developed; however, it lacks dimensional consistency. Patole and Kulkarni [11] investigated surface roughness in the minimum quantity lubrication (MQL) turning of AISI 4340 alloy steel using coated carbide cutting tools and a multi-walled carbon nanotube nanofluid. A full factorial design was employed to examine the effects of cutting speed, feed, depth of cut, and corner radius. Analysis of variance (ANOVA) revealed feed as the most significant factor influencing surface roughness. A quadratic regression model was subsequently developed using response surface methodology (RSM). However, like many empirical models, it lacks dimensional consistency. Zerti et al. [12] investigated the application of grey relational analysis (GRA) based on a Taguchi design for the simultaneous optimization of surface quality and productivity in the dry turning of AISI D3 steel with mixed ceramic cutting tools. The experiments were designed using a Taguchi L18 orthogonal array, considering five control factors: major cutting edge angle, corner radius, cutting speed, feed, and depth of cut. Analysis of variance (ANOVA) revealed that feed and corner radius were the most significant factors affecting surface roughness. A linear regression model with interactions was developed to predict surface roughness; however, the resulting model lacks dimensional consistency. Patel and Gandhi [13] investigated surface roughness in the hard turning of AISI D2 steel with cubic boron nitride (CBN) cutting tools, considering the effects of cutting speed, feed, and corner radius while maintaining a constant depth of cut. Analysis of variance (ANOVA) revealed that feed had the most significant influence on surface roughness, followed by cutting speed and corner radius. A power-law regression model was proposed; however, it lacks dimensional consistency. Saidi et al. [14] investigated surface roughness in the turning of cobalt-based Stellite 6 alloy with

coated carbide cutting tools. The experiments were designed using a Taguchi L27 orthogonal array, with cutting speed, feed, depth of cut, and corner radius as control factors. Analysis of variance (ANOVA) and Pareto analysis indicated that feed and corner radius were the statistically significant factors. A quadratic regression model was developed; however, the resulting model lacks dimensional consistency. Ozdemir [15] investigated surface roughness in the turning of St 37 steel with coated carbide cutting tools using a Taguchi L27 orthogonal array. Cutting speed, feed, depth of cut, and corner radius were selected as control factors. Analysis of variance (ANOVA) revealed that feed had the most significant influence, followed by corner radius and depth of cut. A quadratic regression model was developed; however, the resulting model lacks dimensional consistency. Frifita et al. [16] investigated surface roughness in the turning of nickel-base superalloy Inconel 718 with coated carbide cutting tools using a Taguchi L18 orthogonal array. Cutting speed, feed, and corner radius were selected as control factors. Analysis of variance (ANOVA) revealed that all three control factors were statistically significant. A linear regression model with interaction terms was developed; however, the resulting model lacks dimensional consistency. Ky [17] investigated surface roughness in the hard turning of SAE 420 steel with coated cubic boron nitride (CBN) cutting tools using a central composite design (CCD). Cutting speed, feed, depth of cut, and corner radius were selected as control factors. Analysis of variance (ANOVA) was performed to determine their influence on surface roughness, revealing that cutting speed, feed, and corner radius were statistically significant. A quadratic regression model was proposed; however, the resulting model lacks dimensional consistency. Tomov et al. [18] investigated surface roughness in the turning of EN C55 steel (53 HRC) with cubic boron nitride (CBN) cutting tools using a full factorial design. Cutting speed, feed, depth of cut, and corner radius were selected as control factors. Analysis of variance (ANOVA) revealed that corner radius and feed were the statistically significant factors. A power-law regression model was developed; however, the resulting model lacks dimensional consistency. Lu et al. [19] investigated surface roughness in the turning of AISI 1045 steel with coated carbide cutting tools using a Box–Behnken design. Cutting speed, feed, depth of cut, and corner radius were selected as control factors. Analysis of variance (ANOVA) indicated that feed and corner radius were the statistically significant factors. A linear regression model was developed to correlate actual and theoretical surface roughness. The proposed model is dimensionally consistent.

The reviewed studies consistently identified corner radius and feed as the most influential control factors affecting surface roughness. Surface roughness was typically modeled using regression analysis, with equations taking the form of linear, linear with interactions, quadratic, or power-law functions.

3. THEORETICAL MODELS OF SURFACE ROUGHNESS

Theoretically, surface roughness can be predicted if the cutting tool tip geometry and the feed are known. Theoretical average maximum height of the profile (Rz_{th}) and theoretical roughness average (Ra_{th}) for a cutting tool with a rounded tip can be determined using the classical circle model (Figure 1).

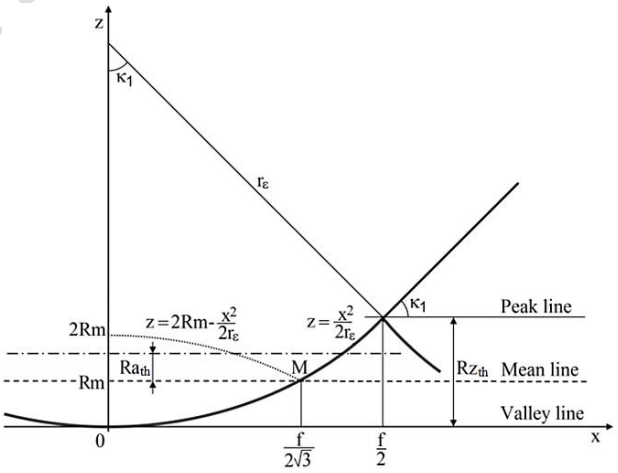

Fig. 1. Idealized model of surface roughness for a cutting tool with a rounded tip.

3.1 Theoretical model for predicting average maximum height of the profile (Rz_{th})

Based on the idealized model of surface roughness for a cutting tool with a rounded tip, shown in Figure 1, it is

$$Rz_{th} = r_{\varepsilon} - \sqrt{r_{\varepsilon}^2 - \frac{f^2}{4}}$$

$$Rz_{th} \approx \frac{f^2}{8r_\varepsilon} \quad (1)$$

Where: Rz_{th} is the theoretical average maximum height of the profile (mm), f is the feed (mm/rev), and r_ε is the corner radius (mm).
The equation is valid for:

$$f \le 2r_\varepsilon \cdot \sin\kappa_1 \quad (2)$$

Where: κ_1 is the minor cutting edge angle (°).

3.2 Theoretical model for predicting roughness average Ra_{th}

The equation of the circle in the x–z coordinate system is:

$$(r_\varepsilon - z)^2 + x^2 = r_\varepsilon^2$$

$$z^2 - 2r_\varepsilon z + x^2 = 0$$

For small values of z squared ($z^2 \approx 0$) it is:

$$z \approx \frac{x^2}{2r_\varepsilon}$$

The equation of the mean line is:

$$Rm \cdot \frac{f}{2} = \int_0^{f/2} z\,dx = \int_0^{f/2} \frac{x^2}{2r_\varepsilon}\,dx = \frac{1}{2r_\varepsilon} \cdot \frac{x^3}{3}\Big|_0^{f/2} = \frac{1}{6r_\varepsilon} \cdot \frac{f^3}{8} = \frac{f^3}{48r_\varepsilon}$$

$$Rm = \frac{f^2}{24r_\varepsilon}$$

The coordinates of point M(x_M, z_M) are:

$$x_M = \sqrt{2r_\varepsilon z_M} = \sqrt{2r_\varepsilon \cdot \frac{f^2}{24r_\varepsilon}} = \frac{f}{2\sqrt{3}}$$

$$z_M = Rm = \frac{f^2}{24r_\varepsilon}$$

Then, the equation for the theoretical roughness average (Ra_{th}) can be determined.

$$Ra_{th} \cdot \frac{f}{2} = \left[\int_0^{f/(2\sqrt{3})} \left(2Rm - \frac{x^2}{2r_\varepsilon}\right)dx - Rm \cdot \frac{f}{2\sqrt{3}}\right] + \left[\int_{f/(2\sqrt{3})}^{f/2} \frac{x^2}{2r_\varepsilon}dx - Rm\left(\frac{f}{2} - \frac{f}{2\sqrt{3}}\right)\right]$$

$$Ra_{th} \cdot \frac{f}{2} = \left[2Rm \cdot \frac{f}{2\sqrt{3}} - \frac{1}{6r_\varepsilon} \cdot \frac{f^3}{24\sqrt{3}} - Rm \cdot \frac{f}{2\sqrt{3}}\right] + \left[\frac{1}{6r_\varepsilon}\left(\left(\frac{f}{2}\right)^3 - \left(\frac{f}{2\sqrt{3}}\right)^3\right) - Rm \cdot \frac{f}{2} + Rm \cdot \frac{f}{2\sqrt{3}}\right]$$

$$Ra_{th} \cdot \frac{f}{2} = Rm \cdot \frac{f}{\sqrt{3}} - Rm \cdot \frac{f}{2} - \frac{1}{6r_\varepsilon} \cdot \frac{f^3}{12\sqrt{3}} + \frac{1}{6r_\varepsilon} \cdot \frac{f^3}{8}$$

$$Ra_{th} \cdot \frac{f}{2} = \frac{f^2}{24r_\varepsilon} \cdot \frac{f}{\sqrt{3}} - \frac{f^2}{24r_\varepsilon} \cdot \frac{f}{2} - \frac{1}{6r_\varepsilon} \cdot \frac{f^3}{12\sqrt{3}} + \frac{1}{6r_\varepsilon} \cdot \frac{f^3}{8}$$

$$Ra_{th} \cdot \frac{f}{2} = \frac{1}{36\sqrt{3}} \cdot \frac{f^3}{r_\varepsilon}$$

$$Ra_{th} = \frac{1}{18\sqrt{3}} \cdot \frac{f^2}{r_\varepsilon} \quad (3)$$

Where: Ra_{th} is the theoretical roughness average (mm), f is the feed (mm/rev), and r_ε is the corner radius (mm).

The difference between theoretical roughness models for sharp-tip and rounded-tip tools is shown in Table 2.

Table 2. Theoretical models for predicting surface roughness.

Tool	Theoretical model	
	Rz_{th} and Ra_{th} (mm)	Rz_{th} and Ra_{th} (μm)
Sharp-tip tool	$Rz_{th} = \frac{f}{\cot\kappa + \cot\kappa_1}$ $Ra_{th} = \frac{Rz_{th}}{4}$	$Rz_{th} = 1000\frac{f}{\cot\kappa + \cot\kappa_1}$ $Ra_{th} = 250\frac{f}{\cot\kappa + \cot\kappa_1}$
Rounded -tip tool	$Rz_{th} = \frac{f^2}{8r_\varepsilon}$ $Ra_{th} = \frac{1}{18\sqrt{3}}\frac{f^2}{r_\varepsilon}$	$Rz_{th} = 125\frac{f^2}{r_\varepsilon}$ $Ra_{th} = 32.075\frac{f^2}{r_\varepsilon}$
Where: Rz_{th} is the theoretical average maximum height of the profile, Ra_{th} is the theoretical roughness average, f is the feed (mm/rev), r_ε is the nose radius (mm), κ is the cutting edge angle (°), κ_1 is the minor cutting edge angle (°).		

In practical machining, the tip of a cutting tool is never sharp. Even a cutting tool with a sharp tip still has a small edge. When the tip of a tool is very sharp, it quickly wears out, becomes dull, and turns into a small edge. Cutting inserts are manufactured with a rounded tip.

According to theoretical equations for predicting surface roughness, the corner radius (r_ε) and the feed (f) are the most influential factors affecting surface roughness.

4. SEMI-EMPIRICAL MODEL OF SURFACE ROUGHNESS

Dimensional analysis was employed to develop a mathematically dimensionally consistent model. The basis of dimensional analysis is the principle of dimensional homogeneity, which requires that the dimensions on the left-hand side of an equation match those on the right-hand side. While dimensional analysis does not determine the exact form of the equation, it establishes its general structure. The most commonly used tool in dimensional analysis is Buckingham's π theorem. This theorem allows the relationships between variables to be expressed in a dimensionless form through dimensionless products, or π-terms, and enables the reduction of the number of variables. Buckingham's π theorem states: *If there is* k *variables (both independent and dependent) involved in a physical phenomenon, and these variables contain* m *fundamental dimensions (such as M, L, and T), then the variables can be grouped into (k–m) dimensionless products. Each product is called a π-term.* The Greek letter π is used to denote these dimensionless products.

4.1 Simplified semi-empirical model of surface roughness

The simplified surface roughness model considers two control factors: corner radius (r_ε) and feed (f). Theoretical considerations indicate that both factors have a significant influence on surface roughness. Accordingly, surface roughness (Ra) can be expressed as a function of corner radius and feed.

$$Ra = \varphi(r_\varepsilon, f) \tag{4}$$

where Ra is the surface roughness, r_ε is the corner radius, f is the feed, and φ represents an unknown functional relationship.

The model formulation is based on dimensional analysis using the method of repeating variables. The variables involved in the analysis are surface roughness (Ra), corner radius (r_ε), and feed (f), all of which have the same fundamental dimension of length (L). As a result, two independent dimensionless products (π-terms) are obtained. Selecting the corner radius (r_ε) as the repeating variable, the resulting dimensionless groups can be expressed as:

$$\pi_1 = \frac{Ra}{r_\varepsilon} \tag{5}$$

$$\pi_2 = \left(\frac{f}{r_\varepsilon}\right)^2 \tag{6}$$

The functional relationship between the dimensionless products is therefore written as:

$$\pi_1 = \varphi(\pi_2) \tag{7}$$

Substituting the expressions for the π-terms gives the simplified semi-empirical surface roughness model in dimensionless form:

$$\frac{Ra}{r_\varepsilon} = \varphi\left[\left(\frac{f}{r_\varepsilon}\right)^2\right] \tag{8}$$

Solving for surface roughness gives the simplified semi-empirical model in dimensional form:

$$Ra = r_\varepsilon \cdot \varphi\left[\left(\frac{f}{r_\varepsilon}\right)^2\right] \tag{9}$$

Similarly, using f as the repeating variable, the following equations can be obtained:

$$\frac{Ra}{f} = \varphi'\left(\frac{f}{r_\varepsilon}\right) \tag{10}$$

$$Ra = f \cdot \varphi'\left(\frac{f}{r_\varepsilon}\right) \tag{11}$$

4.2 Extended semi-empirical model of surface roughness

In this case, four control factors were considered: corner radius (r_ε), depth of cut (a_p), feed (f), and cutting speed (v_c).

Surface roughness (Ra) is expressed as a function:

$$Ra = \varphi(r_\varepsilon, a_p, f, v_c, a_{p,rec}, f_{rec}, v_{c,rec}) \tag{12}$$

where Ra is the surface roughness, r_ε is the corner radius, a_p is the depth of cut, f is the feed, v_c is the cutting speed, and φ represents an unknown functional relationship. Recommended values for the cutting parameters provided by the tool manufacturer—$a_{p,rec}$, f_{rec}, $v_{c,rec}$—were also considered to normalize the process factors.

Using Buckingham's π-theorem, the model was formulated in π-terms. The dimensionless ratios $a_p/a_{p,rec}$, f/f_{rec}, and $v_c/v_{c,rec}$ were treated as independent π-terms. Considering the remaining variables (Ra, r_ε, f), two additional dimensionless groups were derived using r_ε as the repeating variable. The resulting π-terms are expressed as:

$$\pi_1 = \frac{Ra}{f^2 / r_\varepsilon} \quad (13)$$

$$\pi_2 = \frac{a_p}{a_{p,rec}} \quad (14)$$

$$\pi_3 = \frac{f}{f_{rec}} \quad (15)$$

$$\pi_4 = \frac{v_c}{v_{c,rec}} \quad (16)$$

The relationship between the π-terms can be written as:

$$\pi_1 = \varphi(\pi_2, \pi_3, \pi_4) \quad (17)$$

Substituting the expressions for the π-terms gives the extended semi-empirical surface roughness model in dimensionless form:

$$\frac{Ra}{f^2 / r_\varepsilon} = \varphi\left(\frac{a_p}{a_{p,rec}}, \frac{f}{f_{rec}}, \frac{v_c}{v_{c,rec}}\right) \quad (18)$$

Solving for surface roughness gives the extended semi-empirical model in dimensional form:

$$Ra = \frac{f^2}{r_\varepsilon}\varphi\left(\frac{a_p}{a_{p,rec}}, \frac{f}{f_{rec}}, \frac{v_c}{v_{c,rec}}\right) \quad (19)$$

5. EXPERIMENTATION

The primary objective of the experiment is to analyze the influence of selected factors on surface roughness and to identify those that have a significant impact. These factors, which can potentially affect surface roughness, are selected based on theoretical considerations, a literature review, practical experience, and the feasibility of variation and measurement within the experiment. The form of the mathematical model for predicting surface roughness depends on the selected factors. Four factors were selected for predicting surface roughness: corner radius (r_ε), depth of cut (a_p), feed (f), and cutting speed (v_c). Each factor was assigned four levels. Surface roughness, quantified as the roughness average (Ra), was selected as the response. Surface roughness (Ra) was measured with a Mitutoyo SurfTest SJ-301 profilometer (evaluation length 2.5 mm, cutoff 0.8 mm). The secondary objective is to use the experimental data to determine the unknown coefficients and exponents in the mathematical model. The experimental design was based on Taguchi's methodology, which emphasizes efficient and systematic investigation of multiple factors with a reduced number of runs. The study examined the effects of four factors, each varied across four distinct levels. To accommodate this setup, a standard L16 orthogonal array was employed, requiring a total of 16 experimental runs. This particular array was selected because it is specifically suited for four-level factors and allows for a balanced and orthogonal investigation of the factor space. The L16 orthogonal array is designed to provide independent estimation of only the main effects of the factors. Due to the structure of the array and the limited number of degrees of freedom available, no degrees of freedom remain to estimate potential interaction effects between factors. Any interaction effects are confounded with experimental error. This limitation represents a compromise between experimental economy and the ability to detect interaction effects. The experimental conditions are presented in Table 3, the factors and their levels in Table 4, and the experimental design and results in Table 5.

Table 3. Experimental conditions

Category	Parameter	Details
Machining method	Turning	Longitudinal, external
Workpiece	Material	Stainless steel AISI 316 LVM
	Size	ϕ12x120 mm
Machine tool	Lathe	Universal PA-C30 (Potisje, Ada, Serbia)
	Power	P_c=11 kW
	Spindle speed range	n=20-2000 rpm
	Feed range	f=0.04-9.136 mm/rev
Cutting tool	Holder	PCLNR 3225P12
	Insert	CNMG120404-MF: a_p=0.4 mm (0.1-1.5), f=0.15 mm/rev (0.05-0.3), v_c=275 m/min (210-320) CNMG120408-MM: a_p=3 mm (0.5-5.7), f=0.25 mm/rev (0.1-0.45), v_c=230 m/min (170-300) CNMG120412-MR: a_p=3 mm (2-7.6), f=0.35 mm/rev (0.15-0.6), v_c=195 m/min (140-275) CNMG120416-MR: a_p=3 mm (2-7.6), f=0.4 mm/rev (0.15-0.7), v_c=180 m/min (130-275)
	Insert material	Coated carbide
	Coating	CVD TiCN+Al_2O_3+TiN
	Grade	GC2015 (Sandvik Coromant)
Cutting environment	Dry cutting	

Table 4. Factors and levels.

Factor	Symbol	Levels				Unit
Corner radius	r_ε	0.4	0.8	1.2	1.6	mm
Depth of cut	a_p	0.4	0.5	0.6	0.7	mm
Feed	f	0.098	0.107	0.124	0.142	mm/rev
Cutting speed	v_c	22.608	27.883	34.289	41.448	m/min

Table 5. Experimental design and results.

Run	Factors				Response			
	r_ε (mm)	a_p (mm)	f (mm/rev)	v_c (m/min)	Ra_1 (µm)	Ra_2 (µm)	Ra_3 (µm)	Ra_{avg} (µm)
1	0.4	0.4	0.098	22.608	1.16	1.20	1.15	1.17
2	0.4	0.5	0.107	27.883	1.31	1.47	1.53	1.44
3	0.4	0.6	0.124	34.289	1.96	1.95	1.92	1.94
4	0.4	0.7	0.142	41.448	2.24	2.54	2.30	2.36
5	0.8	0.4	0.107	34.289	0.64	0.65	0.69	0.66
6	0.8	0.5	0.098	41.448	0.59	0.61	0.66	0.62
7	0.8	0.6	0.142	22.608	1.13	1.14	1.20	1.16
8	0.8	0.7	0.124	27.883	0.80	0.85	0.86	0.84
9	1.2	0.4	0.124	41.448	0.50	0.55	0.48	0.51
10	1.2	0.5	0.142	34.289	0.85	0.97	0.93	0.92
11	1.2	0.6	0.098	27.883	0.36	0.34	0.38	0.36
12	1.2	0.7	0.107	22.608	0.42	0.41	0.39	0.41
13	1.6	0.4	0.142	27.883	0.59	0.57	0.50	0.55
14	1.6	0.5	0.124	22.608	0.42	0.41	0.45	0.43
15	1.6	0.6	0.107	41.448	0.39	0.34	0.35	0.36
16	1.6	0.7	0.098	34.289	0.28	0.31	0.32	0.30

A main effects plot (Figure 2) was generated to analyze the influence of the factors. The steep lines indicate that corner radius and feed significantly affect surface roughness, while the relatively flat lines show that depth of cut and cutting speed have a minor effect.

ANOVA was performed to assess factor effects on surface roughness; results are presented in Table 6.

The results indicate that surface roughness (Ra) is significantly influenced by corner radius (r_ε) and feed (f), as their p-values are less than 0.05. The corner radius is the most influential factor, followed by the feed. The corner radius contributes 77.10%, while the feed contributes 17.26%.

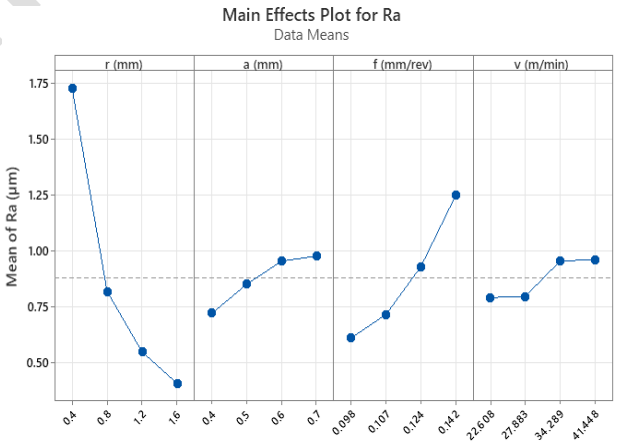

Fig. 2. Main effects plot for surface roughness.

Table 6. Analysis of variance (ANOVA).

Source	DF	SS	MS	F	p	%
r_ε	3	4.20647	1.40216	113.32	0.001	77.10
a_p	3	0.16262	0.05421	4.38	0.128	2.98
f	3	0.94192	0.31397	25.38	0.012	17.26
v_c	3	0.10742	0.03581	2.89	0.203	1.97
Error	3	0.03712	0.01237			0.68
Total	15	5.45554				

Where: DF is the degrees of freedom, SS is the sum of squares, MS is the mean square, F is the variance ratio, p is the probability value, and % is the percent contribution.

5.1. Simplified surface roughness model

ANOVA results indicate that corner radius (r_ε) and feed (f) significantly influence surface roughness (Ra). Surface roughness is modeled using the simplified semi-empirical model expressed in dimensionless form, as given in Equation 7. The calculated values of $\pi_1=Ra/r_\varepsilon$, and $\pi_2=(f/r_\varepsilon)^2$, for all experimental runs are presented in Table 7.

Table 7. Calculated values of $\pi_1=Ra/r_\varepsilon$ and $\pi_2=(f/r_\varepsilon)^2$.

Exp. run	r_ε (mm)	f (mm/rev)	Ra (mm)	$\pi_2=(f/r_\varepsilon)^2$	$\pi_1=Ra/r_\varepsilon$
1	0.4	0.098	0.00117	0.060025	0.002925
2	0.4	0.107	0.00144	0.071556	0.003600
3	0.4	0.124	0.00194	0.096100	0.004850
4	0.4	0.142	0.00236	0.126025	0.005900
5	0.8	0.098	0.00062	0.015006	0.000775
6	0.8	0.107	0.00066	0.017889	0.000825
7	0.8	0.124	0.00084	0.024025	0.001050
8	0.8	0.142	0.00116	0.031506	0.001450
9	1.2	0.098	0.00036	0.006669	0.000300
10	1.2	0.107	0.00041	0.007951	0.000342
11	1.2	0.124	0.00051	0.010678	0.000425
12	1.2	0.142	0.00092	0.014003	0.000767
13	1.6	0.098	0.00030	0.003752	0.000188
14	1.6	0.107	0.00036	0.004472	0.000225
15	1.6	0.124	0.00043	0.006006	0.000269
16	1.6	0.142	0.00055	0.007877	0.000344

The relationship between $\pi_1=Ra/r_\varepsilon$ and $\pi_2=(f/r_\varepsilon)^2$ is shown in Figure 3.

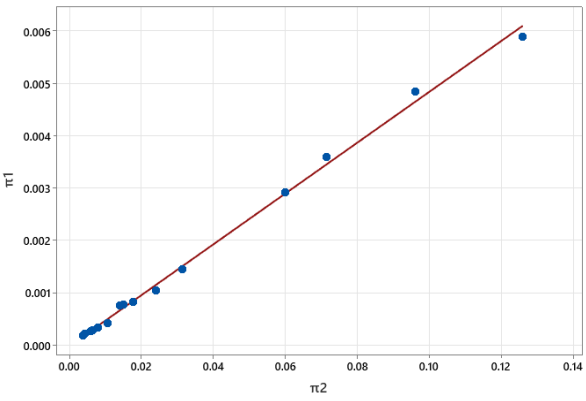

Fig. 3. Relationship between $\pi_1=Ra/r_\varepsilon$ and $\pi_2=(f/r_\varepsilon)^2$

The dimensionless equation (7) was fitted using linear regression, resulting in a coefficient of determination of $R^2 = 0.997$.

$$\pi_1 = 0.048\pi_2 \tag{20}$$

The dimensionless equation is:

$$\frac{Ra}{r_\varepsilon} = 0.048\left(\frac{f}{r_\varepsilon}\right)^2 \tag{21}$$

The surface roughness dimensional equation is:

$$Ra = 0.048\frac{f^2}{r_\varepsilon} \tag{22}$$

Where: Ra is the surface roughness (mm), f is the feed (mm/rev), r_ε is the corner radius (mm).
Since Ra is expressed in micrometers, the simplified surface roughness model is:

$$Ra = 48\frac{f^2}{r_\varepsilon} \tag{23}$$

Where: Ra is the surface roughness (μm).

5.2. Extended surface roughness model

Surface roughness is modeled using an extended semi-empirical model expressed in dimensionless form, as given in Equation 17.

The calculated values of $\pi_1=Ra/(f^2/r_\varepsilon)$, $\pi_2=a_p/a_{p,rec}$, $\pi_3=f/f_{rec}$, and $\pi_4=v_c/v_{c,rec}$, for all experimental runs are presented in Table 8.

Table 8. Calculated values of $\pi_1=Ra/(f^2/r_\varepsilon)$, $\pi_2=a_p/a_{p,rec}$, $\pi_3=f/f_{rec}$, and $\pi_4=v_c/v_{c,rec}$.

Exp. run	r_ε (mm)	a_p (mm)	$a_{p,rec}$ (mm)	f (mm/rev)	f_{rec} (mm/rev)	v_c (m/min)	$v_{c,rec}$ (m/min)	Ra (mm)	$\pi_2=a_p/a_{p,rec}$	$\pi_3=f/f_{rec}$	$\pi_4=v_c/v_{c,rec}$	$\pi_1=Ra/(f^2/r_\varepsilon)$
1	0.4	0.4	0.4	0.098	0.15	22.608	275	0.00117	1.000	0.653	0.082211	0.048730
2	0.4	0.5	0.4	0.107	0.15	27.883	275	0.00144	1.250	0.713	0.101393	0.050310
3	0.4	0.6	0.4	0.124	0.15	34.289	275	0.00194	1.500	0.827	0.124687	0.050468
4	0.4	0.7	0.4	0.142	0.15	41.448	275	0.00236	1.750	0.947	0.150720	0.046816
5	0.8	0.4	3	0.098	0.25	34.289	230	0.00062	0.133	0.392	0.149083	0.051645
6	0.8	0.5	3	0.107	0.25	41.448	230	0.00066	0.167	0.428	0.180209	0.046118
7	0.8	0.6	3	0.124	0.25	22.608	230	0.00084	0.200	0.496	0.098295	0.043704
8	0.8	0.7	3	0.142	0.25	27.883	230	0.00116	0.233	0.568	0.121230	0.046023
9	1.2	0.4	3	0.098	0.35	41.448	195	0.00036	0.133	0.280	0.212554	0.044981
10	1.2	0.5	3	0.107	0.35	34.289	195	0.00041	0.167	0.306	0.175841	0.042973
11	1.2	0.6	3	0.124	0.35	27.883	195	0.00051	0.200	0.354	0.142990	0.039802
12	1.2	0.7	3	0.142	0.35	22.608	195	0.00092	0.233	0.406	0.115938	0.054751
13	1.6	0.4	3	0.098	0.4	27.883	180	0.00030	0.133	0.245	0.154906	0.049980
14	1.6	0.5	3	0.107	0.4	22.608	180	0.00036	0.167	0.267	0.125600	0.050310
15	1.6	0.6	3	0.124	0.4	41.448	180	0.00043	0.200	0.310	0.230267	0.044745
16	1.6	0.7	3	0.142	0.4	34.289	180	0.00055	0.233	0.355	0.190494	0.043642

The dimensionless equation (17) was fitted to the experimental data using power-law regression.

$$\pi_1 = 0.037\pi_2^{0.031}\pi_3^{-0.064}\pi_4^{-0.116} \tag{24}$$

The dimensionless equation is:

$$\frac{Ra}{f^2/r_\varepsilon} = 0.037\left(\frac{a_p}{a_{p,rec}}\right)^{0.031}\left(\frac{f}{f_{rec}}\right)^{-0.064}\left(\frac{v_c}{v_{c,rec}}\right)^{-0.116} \tag{25}$$

For model validation, the percent error for each test run was calculated using the following formula:

$$Error(\%) = \left|\frac{\pi_{1,\exp}-\pi_{1,pred}}{\pi_{1,\exp}}\right|\cdot 100\% \tag{26}$$

Where: $\pi_{1,exp}$ is the π value based on experimental data, and $\pi_{1,pred}$ is the predicted π value.

The percent errors for model validation are summarized in Table 9, with an average error of 5.54%.

Table 9. Percent errors for model validation.

Run	$\pi_{1,exp}$	$\pi_{1,pred}$	Error (%)
1	0.048730	0.050806	4.26
2	0.050310	0.049649	1.31
3	0.050468	0.048286	4.32
4	0.046816	0.047052	0.50
5	0.051645	0.046021	10.90
6	0.046118	0.045084	2.24
7	0.043704	0.048182	10.25
8	0.046023	0.046839	1.77
9	0.044981	0.045127	0.32
10	0.042973	0.046194	7.49
11	0.039802	0.047139	18.43
12	0.054751	0.048105	12.14
13	0.049980	0.047216	5.53
14	0.050310	0.048454	3.69
15	0.044745	0.044985	0.54
16	0.043642	0.045805	4.96
Avg			5.54

The surface roughness dimensional equation is:

$$Ra = 0.037\frac{f^2}{r_\varepsilon}\left(\frac{a_p}{a_{p,rec}}\right)^{0.031}\left(\frac{f}{f_{rec}}\right)^{-0.064}\left(\frac{v_c}{v_{c,rec}}\right)^{-0.116} \tag{27}$$

Where: Ra is the surface roughness (mm), r_ε is the corner radius (mm), a_p is the depth of cut (mm), $a_{p,rec}$ is the recommended depth of cut (mm), f is the feed (mm/rev), f_{rec} is the recommended feed

(mm/rev), v_c is the cutting speed (m/min), and $v_{c,rec}$ is the recommended cutting speed (m/min). Since *Ra* is expressed in micrometers, the extended surface roughness model is:

$$Ra = 37\frac{f^2}{r_\varepsilon}\left(\frac{a_p}{a_{p,rec}}\right)^{0.031}\left(\frac{f}{f_{rec}}\right)^{-0.064}\left(\frac{v_c}{v_{c,rec}}\right)^{-0.116} \quad (28)$$

Where: *Ra* is the surface roughness (μm).
The developed mathematical models are valid strictly within the defined experimental domain and operational assumptions of this study.

6. CONCLUSION

A semi-empirical, dimensionless model for predicting surface roughness in finish turning of AISI 316LVM stainless steel was developed by integrating dimensional analysis (Buckingham's π theorem), design of experiments, and regression analysis. Analysis of variance confirmed that corner radius and feed are the dominant factors while depth of cut and cutting speed showed a minor influence on surface roughness. In agreement with existing models reported in the literature, the proposed simplified surface roughness model confirms the predominant role of corner radius and feed in controlling surface roughness in turning operations. The present work differs from most published models in several key aspects. Unlike purely empirical regression models for surface roughness, which rely on absolute values of cutting parameters and are often dimensionally inconsistent, the proposed models are strictly dimensionally homogeneous, ensuring physical consistency. The proposed extended surface roughness model introduces normalized cutting parameters based on tool manufacturer's recommendations. This approach represents a novel contribution and enhances industrial applicability. Two surface roughness models were developed: a simplified model that includes corner radius and feed as factors, and an extended model that includes corner radius, feed, depth of cut, and cutting speed as factors. The simplified surface roughness model, expressed as a linear regression equation, showed excellent agreement with the experimental data, with a coefficient of determination of R^2 = 0.997. The extended surface roughness model, expressed as a power-law regression equation, demonstrated reliable performance, with an average error of 5.54%. This successful validation confirms that both models provide quantitatively accurate and physically consistent predictions of surface roughness within the specified range of machining conditions. Overall, the proposed approach combines the strengths of existing empirical models with the rigor of dimensional analysis, offering improved interpretability, robustness, and practical relevance. Future work should focus on incorporating tool wear, vibration, and validating the models for other materials and machining environments.

REFERENCES

[1] ASME B46.1, *Surface Texture (Surface Roughness, Waviness, and Lay)*, 2009.

[2] C. Mahajan, M. Mote, B. Patil, H. Patil, and M. Phate, "Formulation and Simulation of a Field Data Based Model for the Turning Process by Using Response Surface Method", *International Journal of Advanced Scientific and Technical Research,* vol. 2, issue 3, pp. 355-370, 2013.

[3] J. Stanojkovic, M. Madic, M. Trifunovic, P. Jankovic, D. Petkovic, "A novel approach to predicting the cutting force in turning using dimensional analysis", *Facta Universitatis, Series: Mechanical Engineering*, 2025, doi: 10.22190/FUME241129010S.

[4] S. Bazaz, J. Ratava, M. Lohtander, and J. Varis, "An Investigation of Factors Influencing Tool Life in the Metal Cutting Turning Process by Dimensional Analysis", *Machines*, vol. 11, 393, 2023, doi: 10.3390/machines11030393.

[5] M. Modi, V. Patil, A. Sharma, V. Sharma, Y Joshi, A. Jain, S. Chodhary, "Empirical Modeling and Comparative Analysis of Lathe Machine", *International Journal of Engineering Applied Sciences and Technology*, vol. 5, issue 2, pp. 435-438, 2020.

[6] D. Singh, and P.V. Rao, "A Surface Roughness Prediction Model for Hard Turning Process", *International Journal of Advanced Manufacturing Technology*, vol. 32, pp. 1115–1124, 2007, doi: 10.1007/s00170-006-0429-2.

[7] N. Qehaja, K. Jakupi, A. Bunjaku, M. Bruci, and H. Osmani, "Effect of Machining Parameters and Machining Time on Surface Roughness in Dry Turning Process", *Procedia Engineering*, vol. 100, pp. 135–140, 2015, doi: 10.1016/j.proeng.2015.01.351.

[8] S. Dinesh, K. Rajaguru, V. Vijayan, and A. Godwin Antony, "Investigation and Prediction of Material Removal Rate and Surface Roughness in CNC Turning of EN24 Alloy Steel", *Mechanics and*

Mechanical Engineering, vol. 20, no. 4, pp. 451–466, 2016, doi: 10.5958/2249-7315.2016.00654.7.

[9] C.O. Izelu, and S.C. Eze, "An Investigation on Effect of Depth of Cut, Feed Rate and Tool Nose Radius on Induced Vibration and Surface Roughness During Hard Turning of 41Cr4 Alloy Steel Using Response Surface Methodology", *International Journal of Engineering and Technologies*, vol. 7, pp. 32–46, 2016, doi: 10.56431/p-08ad20.

[10] I. Meddour, M.A. Yallese, H. Bensouilah, A. Khellaf, and M. Elbah, "Prediction of Surface Roughness and Cutting Forces Using RSM, ANN, and NSGA-II in Finish Turning of AISI 4140 Hardened Steel With Mixed Ceramic Tool", *International Journal of Advanced Manufacturing Technology*, vol. 97, pp. 1931–1949, 2018, doi: 10.1007/s00170-018-2026-6.

[11] P.B. Patole, and V.V. Kulkarni, "Prediction of Surface Roughness and Cutting Force Under MQL Turning of AISI 4340 With Nano Fluid by Using Response Surface Methodology", *Manufacturing Review*, vol. 5, no. 5, 2018, doi: 10.1051/mfreview/2018002.

[12] O. Zerti, M.A. Yallese, A. Zerti, S. Belhadi, and F. Girardin, "Simultaneous Improvement of Surface Quality and Productivity Using Grey Relational Analysis Based Taguchi Design for Turning Couple (AISI D3 Steel/Mixed Ceramic Tool (Al2O3 + TiC))", *International Journal of Industrial Engineering Computations*, vol. 9, pp. 173–194, 2018, doi: 10.5267/j.ijiec.2017.7.001.

[13] V.D. Patel, and A.H. Gandhi, "Analysis and Modeling of Surface Roughness Based on Cutting Parameters and Tool Nose Radius in Turning of AISI D2 Steel Using CBN Tool", *Measurement*, vol. 138, pp. 34-38, 2019, doi:10.1016/j.measurement.2019.01.077.

[14] R. Saidi, B. Fathallah, T. Mabrouki, S. Belhadi, and M. A. Yallese, "Modeling and Optimization of the Turning Parameters of Cobalt Alloy (Stellite 6) Based on RSM and Desirability Function", *International Journal of Advanced Manufacturing Technology*, vol. 100, pp. 2945–2968, 2019, doi: 10.1007/s00170-018-2816-x.

[15] M. Ozdemir, "Modelling and Prediction of Effect of Machining Parameters on Surface Roughness in Turning Operations", *Tehnički vjesnik-Technical Gazette*, vol. 27, no. 3, pp. 751–760, 2020, doi: 10.17559/TV-20190320104114.

[16] W. Frifita, S. Salem, A. Haddad, and M. Yallese, "Optimization of Machining Parameters in Turning of Inconel 718 Nickel-base Superalloy", *Mechanics & Industry*, vol. 21, no. 2, article 203, 2020, doi: 10.1051/meca/2020001.

[17] L.H. Ky, "Surface Roughness Model When Hole Turning SAE 420 Steel", *European Journal of Engineering Research and Science (EJERS)*, vol. 5, issue 6, pp. 683–688, June 2020, doi: 10.24018/ejers.2020.5.6.1966.

[18] M. Tomov, V. Gecevska, and E. Vasileska, "Modeling of Multiple Surface Roughness Parameters During Hard Turning: A Comparative Study Between the Kinematical-Geometrical Copying Approach and the Design of Experiments Method (DOE)", *Advances in Production Engineering & Management*, vol. 17, no. 1, pp. 75–88, 2022, doi: 10.14743/apem2022.1.422.

[19] J. Lu, X. Wang, S. Chen, X. Liao, and K. Chen, "Surface Roughness Prediction for Turning Based on the Corrected Subsection Theoretical Model", *The International Journal of Advanced Manufacturing Technology,* vol. 124, issue 1-2, pp. 21-35, 2023, doi: 10.1007/s00170-022-10471-1.